Chemistry & Biology
Article

A Single Cluster of Coregulated Genes Encodes the Biosynthesis of the Mycotoxins Roquefortine C and Meleagrin in *Penicillium chrysogenum*

Carlos García-Estrada,[1] Ricardo V. Ullán,[1] Silvia M. Albillos,[1] María Ángeles Fernández-Bodega,[1] Pawel Durek,[3,4] Hans von Döhren,[3] and Juan F. Martín[1,2,*]
[1]Instituto de Biotecnología de León (INBIOTEC), Parque Científico de La Granja, Avda. Real, 1, 24006 León, Spain
[2]Departamento de Biología Molecular, Área de Microbiología, Facultad de CC. Biológicas y Ambientales, Universidad de León, Campus de Vegazana, 24071 León, Spain
[3]Department of Chemistry, Technical University Berlin, D-10623 Berlin, Germany
[4]Present address: Institute of Pathology, Universitätmedizin Charité, D-10117 Berlin, Germany
*Correspondence: jf.martin@unileon.es
DOI 10.1016/j.chembiol.2011.08.012

SUMMARY

A single gene cluster of *Penicillium chrysogenum* contains genes involved in the biosynthesis and secretion of the mycotoxins roquefortine C and meleagrin. Five of these genes have been silenced by RNAi. Pc21g15480 (*rds*) encodes a nonribosomal cyclodipeptide synthetase for the biosynthesis of both roquefortine C and meleagrin. Pc21g15430 (*rpt*) encodes a prenyltransferase also required for the biosynthesis of both mycotoxins. Silencing of Pc21g15460 or Pc21g15470 led to a decrease in roquefortine C and meleagrin, whereas silencing of the methyltransferase gene (Pc21g15440; *gmt*) resulted in accumulation of glandicolin B, indicating that this enzyme catalyzes the conversion of glandicolin B to meleagrin. All these genes are transcriptionally coregulated. Our results prove that roquefortine C and meleagrin derive from a single pathway.

INTRODUCTION

Most filamentous fungi produce a variety of chemically diverse secondary metabolites (Jiang and An, 2000; Godio and Martín, 2009). Some are important for medicine, but many others are potent mycotoxins (Yu et al., 1996; Jarvis and Miller, 2005).

Roquefortine C, a member of the diketopiperazine (DKP) alkaloid family, was first isolated from cultures of *Penicillium roqueforti* (Scott and Kennedy, 1976) and later from cultures of other *Penicillium* species growing on contaminated feed grain (Häggblom, 1990; Ohmomo et al., 1994), onions (Overy et al., 2005), beer (Cole et al., 1983), and wine (Möller et al., 1997). Roquefortine C contamination of food and feedstuff is of great interest because of the well-known neurotoxicity of this mycotoxin (Wagener et al., 1980). Toxicological studies supported the initial observations on the toxicity of roquefortine C (Ohmomo, 1982).

Penicillium chrysogenum is a common contaminant of grains, bread, and processed food. Industrially, *P. chrysogenum* is used for penicillin production. Initial experiments in our laboratory showed that *P. chrysogenum* NRRLL 1951 (wild-type) and its derivative Wisconsin 54-1255 (hereafter named Wis54-1255) produce roquefortine C and meleagrin (García-Rico et al., 2008). Natural isolates of *P. chrysogenum* different from the NRRL 1951 strain, produce in addition to roquefortine C, small amounts of 3,12-dihydroroquefortine C (known as roquefortine D) and traces of glandicolines A and B (Vinokurova et al., 2003) and meleagrin (Jarvis, 2003). All these metabolites are structurally closely related (Overy et al., 2005) and may arise from common biosynthetic precursors by late enzymatic modifications. Precursor feeding experiments revealed that tryptophan, histidine, and mevalonate are involved in the biosynthesis of roquefortine C (Barrow et al., 1979; Gorst-Allman et al., 1982). Thus, the DKP precursor of the roquefortine family may be predicted to be formed from tryptophan (or from dimethylallyltryptophan, DMAT) and histidine activated by a two-module nonribosomal peptide synthetase (NRPS). Recent evidence from other DKP alkaloids suggests that the DKP intermediate is then modified by isoprenylation at C3 and ring closure between C2 and N12 (Yin et al., 2009a).

Prenylated indole alkaloids are widely distributed in nature, particularly in filamentous fungi (Stocking et al., 2000; Williams et al., 2000; Li, 2009). Interestingly, prenylated indole alkaloids have diverse chemical structures. The isopentenyl group is present in different prenylated tryptophan derivatives in almost every position of the indole or indoline ring (Li, 2009). In some of the compounds, the prenyl (isopentenyl) moiety is attached to the indole ring in a "reverse" mode, i.e., by a connection via its C3′ carbon atom. A series of natural products carrying reverse prenyl moieties at position C3 of the indoline rings and an additional ring between the indoline and the DKP moieties (or their analogs) were identified in different ascomycetes, e.g., roquefortine C from *Penicillium* strains (Finoli et al., 2001; Rundberget et al., 2004) and acetylaszonalenin from *Aspergillus* and *Neosartorya* strains (Kimura et al., 1982; Wakana et al., 2006; Yin et al., 2009b).

Although roquefortine C production is best characterized in *P. roqueforti*, there is no information on the genes or enzymes involved in roquefortine C biosynthesis. The complete genome of *P. chrysogenum* Wis54-1255 has been sequenced (van den Berg et al., 2008), and this fungus is amenable to gene-silencing techniques (Ullán et al., 2008). The effect of the regulatory protein LaeA and the Gα subunit of the heterotrimeric G protein on

roquefortine C production has been reported in *P. chrysogenum* (García-Rico et al., 2008; Kosalková et al., 2009). Therefore, it was of great interest to study the genes encoding the biosynthesis of roquefortine C and meleagrin in this fungus.

RESULTS

Analysis of the Genetic Region Containing the Putative Roquefortine Prenyltransferase and Dipeptide Synthetase Genes

The *P. chrysogenum* Wis54-1255 genome (van den Berg et al., 2008) contains one ORF (Pc21g15480) that may encode a roquefortine "cyclodipeptide synthetase" (CDPS) with two modules. This ORF is linked to a gene (Pc21g15430) similar to *dmaW* encoding DMAT synthetase (a tryptophan prenyltransferase). This cluster, comprising genes Pc21g15420, Pc21g15430, Pc21g15440, Pc21g15450, Pc21g15460, Pc21g15470, and Pc21g15480 (Figure 1A), is overexpressed in an industrial penicillin-producer strain, but unlike the penicillin biosynthetic genes, it is downregulated after the addition of phenylacetate (see Table S1 available online) (van den Berg et al., 2008).

Amino acid sequence comparison of Pc21g15480 showed strong similarity to fungal NRPSs. The Pc21g15480-encoded protein shows two modules each containing the activation (A), thiolation (T), and condensation (C) domains with a domain structure ATCATC, where the terminal C-domain catalyzes cyclization and release of the peptide (see Discussion). A comparative analysis of available fungal CDPSs has been compiled in Figure S1. Their phylogenetic analysis reveals a clustering in indole-alkaloid-type and epipolythiodioxopiperazine (ETP)-forming enzymes. Pc21g15480 is located in a subcluster with a putative NRPS (59% identity) from *Neosartorya fischeri* NRRL181 (gene ID: 4585978 NFIA_074300) that might synthesize the same DKP alkaloid (see below). Other CDPSs from Aspergilli showed identities below 35%.

The analysis of the predicted substrate-binding pockets of the two adenylation domains of the protein encoded by Pc21g15480 according to the Stachelhaus and Challis algorithm (Lautru and Challis, 2004; Rausch et al., 2005) reveals the motifs DSLELVAVVK and DIAMIGSMYK, which have not been described in any NRPS domain so far.

To analyze the substrate binding in the two adenylate domains, modeling was performed using structures based on the GrsA crystal structure (Schwecke et al., 2006). The fit of L-His and L-Trp has been analyzed; side-chain contacts predicted that the charged His could only be accommodated in the first domain (Figure 2), and thus, the sequence of the initial biosynthetic reactions was established as formation of His' and Trp-adenylates (A1 and A2), followed by thioester attachment (T1 and T2), His-Trp peptide bond formation (C1), and cyclization to cyclo-His-Trp (C2).

Pc21g15430 is similar to *dmaW* encoding a tryptophan prenyltransferase (DMAT synthetase). This protein shows high similarity (81% homology, 67% identity) to the putative DMAT synthetase-like protein from *N. fischeri* (119478629, XP_001259405.1,), to a second DMAT synthetase from *N. fischeri* (119483566, XP_001261686.1n, 70% homology, 50% identity), and also to DMAT synthetases from *Aspergillus fumigatus* (146324647, XP_747143.2, and 159124027, EDP49146.1, 70% homology, 50% identity) and *Aspergillus clavatus* (121704507, XP_001270517.1, 57% homology, 40% identity). The *N. fischeri* NFIA 055310 prenyltransferase has been identified recently as a DKP prenyltransferase (AnaPT) involved in the biosynthesis of acetylaszonalenin (Yin et al., 2009b). A similar role appears to correspond to the *P. chrysogenum* roquefortine prenyltransferase encoded by Pc21g15430 (*rpt*). Thus, reverse prenylation of cyclo-His-Trp in position 3 is likely one of the next biosynthetic steps. The prenylation is followed by the new ring C closure from position 2 of the indole ring to the nitrogen atom of the DKP ring, as described for acetylaszonalenin formation (Yin et al., 2009a), leading to the roquefortine structure. The current state of prenyltransferase functions and the suggested functions for Pc21g15430 have been compiled in Table S2. These correlate with the phylogenetic analysis of these enzymes shown in Figure S2.

Flanking these two ORFs, there are several genes (Figure 1A). Pc21g15420 encodes a probable transporter (highly similar to the cercosporin facilitator protein [CFP]). The encoded protein contains 12 TMSs (transmembrane-spanning segments) that share high similarity to MFS (major facilitator superfamily) transporters from *Penicillium digitatum* (59% identity and 75% homology), *N. fischeri* (55% identity and 73% homology), or *Aspergillus clavatus* (54% identity and 73% homology). Pc21g15440 encodes a protein with high similarity to a putative methyltransferase (see silencing experiments below) of the UbiE/COQ5 family from *A. clavatus* (43% identity and 61% homology) or *N. fischeri* (41% identity and 62% homology). Pc21g15450 codes a protein that shows strong similarity to putative cytochrome P450 monooxygenase (P450l) from *N. fischeri* (66% identity and 79% homology) or *A. clavatus* (64% identity and 79% homology). Pc21g15460 encodes a protein that shows similarity to "maackiain monooxygenase" MAK1 from *N. fischeri* (46% identity and 64% homology) or *A. flavus* (55% homology and 39% identity). Pc21g15470 encodes another protein with high similarity to cytochrome P450 oxygenases from *N. fischeri* (72% homology and 60% identity) or *A. clavatus* (41% identity and 61% homology). Finally, Pc21g15490 encodes a protein with high similarity to a regulatory subunit of protein phosphatase 2a from *A. clavatus* (89% homology and 84% identity) or *N. fischeri* (89% homology and 84% identity). All these genes, except the last one (Pc21g15490), are overexpressed in penicillin-overproducing strains and downregulated in phenylacetate-supplemented medium (van den Berg et al., 2008), suggesting that the seven genes (Pc21g15420 to Pc21g15480) are members of a coregulated cluster, whereas Pc21g15490 may be outside the roquefortine/meleagrin cluster based on the transcriptional data.

Silencing of Pc21g15480 Decreases the Production of Roquefortine C and Meleagrin

It is likely that Pc21g15480 encodes the CDPS in charge of the biosynthesis of roquefortine C. An important question is whether the same CDPS serves for the biosynthesis of both meleagrin and roquefortine C. To test this, Pc21g15480 expression was silenced using the attenuation plasmid pJL43RNAi-*dps*. Transformants were selected with phleomycin. The integration of the attenuation cassette (~1.7 kbp) was confirmed by southern blotting (Figure 3A) in five randomly selected transformants (named

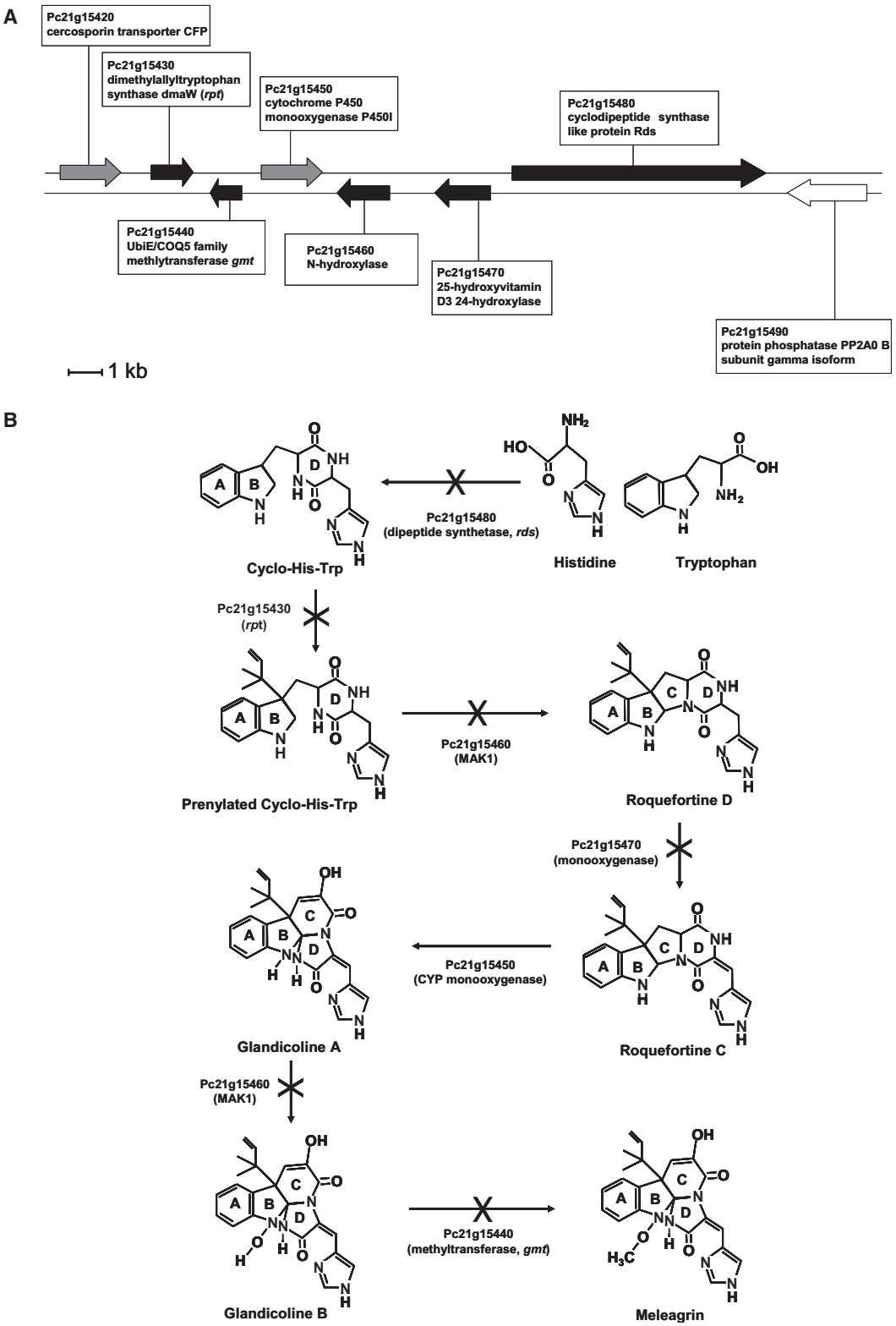

Figure 1. Gene Cluster and Proposed Roquefortine C/Meleagrin Pathway

(A) Schematic representation of the ORFs present in the roquefortine C-meleagrin cluster. ORFs that have been silenced are represented as black arrows. Pc21g15490 (white arrow) is out of the roquefortine/meleagrin cluster (see text). ORFs that have not been silenced are represented as gray arrows.

(B) Proposed biosynthetic pathway in *P. chrysogenum*. Silenced steps are indicated by the symbol ⊣.

See also Figure S2 and Tables S1 and S2.

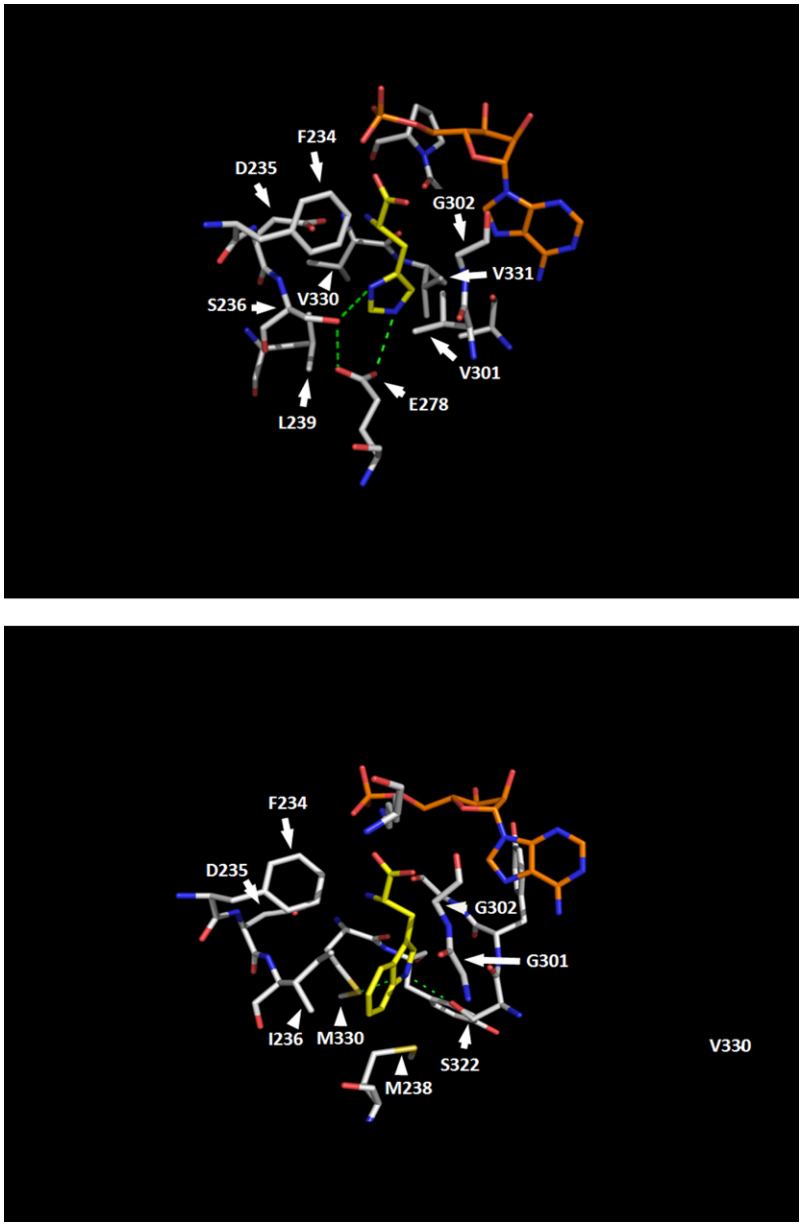

Figure 2. Binding Models of His and Trp in the Catalytic Pockets of Adenylation Domains of the Dipeptide Synthetase Pc21g15480

Modeling was performed by comparison with the GrsA structure (PDB ID: 1Amu) via HHpred and MODELLER. Interacting amino acids were visualized by PyMOL. Numbering of the amino acids corresponds to the respective amino acid numbers of GrsA. The first domain shows a clear preference for His providing H-bondings via SER236 and GLU278 (upper panel), whereas the Trp is presumably bound by the second domain (lower panel). The Trp binding is accomplished through providing additional space for the large Trp molecule by GLY301 in comparison to VAL301 in the first pocket. In addition M330 and S322 are likely to interact with Trp.
See also Figure S1 and Table S3.

B1, B7, B9, B11, and B13). Their DNA was digested with SphI and EcoRI, which cut inside Pc21g15480 releasing a band of 5.5 kbp. The same 444 bp internal fragment used for the attenuation of Pc21g15480 was used as probe. Transformants B11 and B13 were randomly selected for further experimental analysis.

Silencing of the Pc21g15480 gene expression in transformants B11 and B13 was confirmed by qPCR (Figure 3B), and production of roquefortine C and meleagrin was analyzed by HPLC (Figure 3C). As shown in Figure 3D, the production of roquefortine C decreased 63 and 28.4 times, in the two transformants, respectively, when it was compared to the production shown by the parental Wis54-1255 strain. Meleagrin production was also reduced in these transformants between 15 and 33 times, respectively (Figure 3E), as compared to the parental strain. These results suggest that Pc21g15480 encodes a CDPS involved in the biosynthesis of roquefortine C (hereafter named *rds*) and that the same CDPS is required for the biosynthesis of meleagrin.

Silencing of Pc21g15430 Leads to a Drastic Reduction of Both Roquefortine C and Meleagrin Synthesis

In order to test whether the *P. chrysogenum* Pc21g15430 (*rpt*) gene is involved in the biosynthesis of roquefortine C and/or meleagrin, knockdown transformants were obtained. Protoplasts of the Wis54-1255 strain were transformed with plasmid pJL43RNAi-*rpt*. Transformants were selected with phleomycin. Southern blotting was carried out in three randomly selected transformants (named A16, A17, and A18) to confirm the integration of the attenuation cassette in the genome and the integrity of the internal *rpt* gene (Figure 4A). For this purpose, genomic DNA was digested with SphI and EcoRI, which release approximately 1.7 kbp of the attenuation cassette and 0.8 kbp of the internal *rpt* gene. The same 329 bp internal fragment used for the attenuation of the *rpt* gene was used as probe. In all these transformants (Figure 4A), the interference cassette was integrated in the genome without rearrangement of the internal *rpt* gene. Transformants A17 and A18 were used for further experiments.

Silencing of the Pc21g15430 gene expression in transformants A17 and A18 was confirmed by qPCR (Figure 4B), and production of roquefortine C and meleagrin was analyzed by HPLC (Figure 4C). In these transformants the production of roquefortine C was reduced between 15 and 19.3 times, respectively (Figure 4D), when compared to the roquefortine C produced by the parental Wis54-1255 strain. In addition, meleagrin production was also reduced in these transformants between 8.3 and 9.4 times, respectively (Figure 4E), as compared to the parental strain. These results confirmed the participation of the protein encoded by the *rpt* gene in the biosynthesis of roquefortine C and meleagrin.

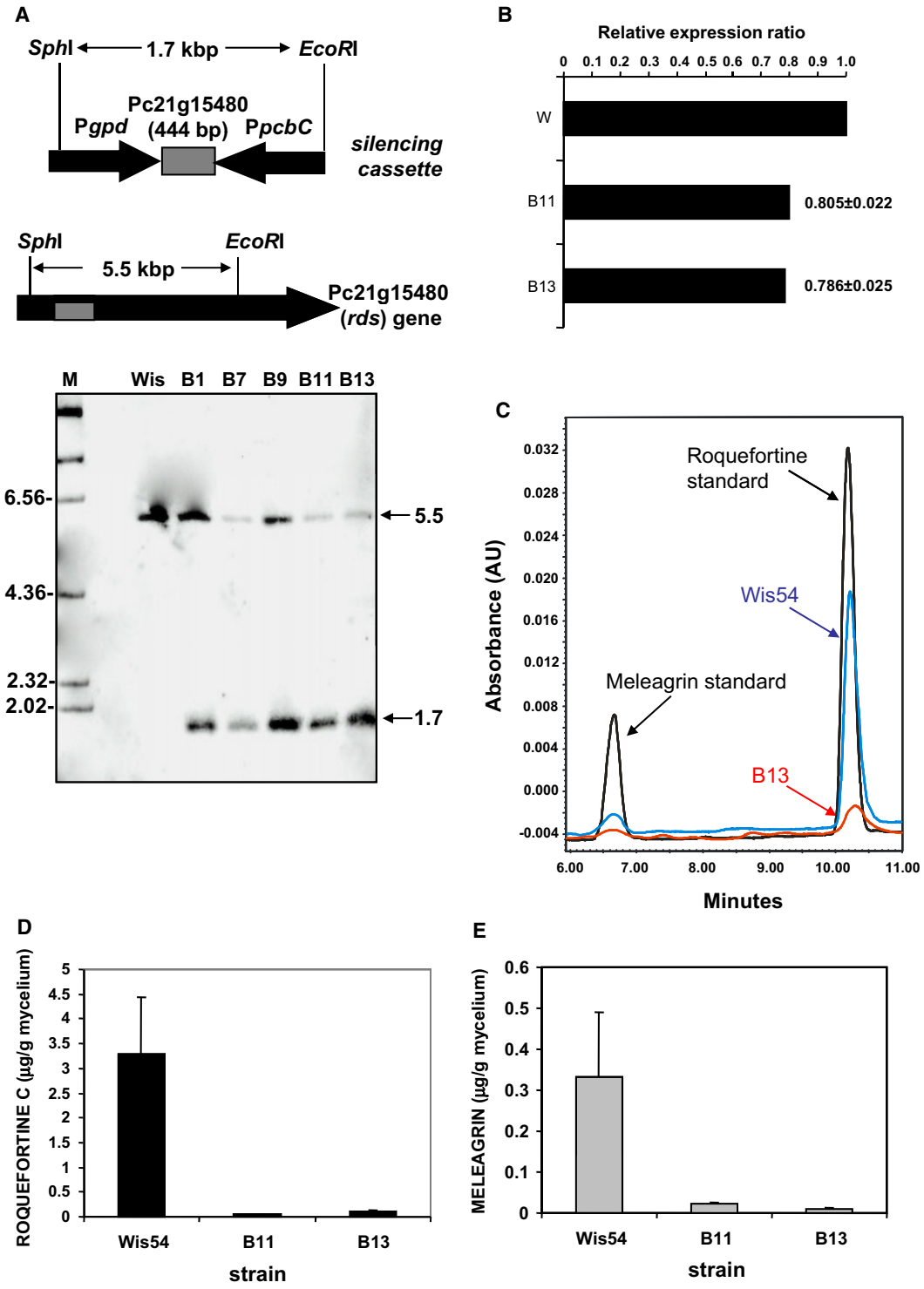

Figure 3. Gene Silencing of Pc21g15480

(A) Southern blot analysis of transformants and the parental *P. chrysogenum* Wis54-1255 (Wis) showing integration of the full silencing cassette (~1.7 kb).

(B) qPCR analysis of the expression of Pc21g15480 in *P. chrysogenum* Wis54-1255 (W) and transformants B11 and B13.

(C) Representative chromatogram showing the meleagrin and roquefortine secreted to the culture medium by transformant B13 and the parental strain Wis54-1255. Pure roquefortine C and meleagrin A standards were added as internal controls.

(D and E) Roquefortine C and meleagrin-specific production (µg/g dry cells), respectively, by transformants B11, B13, and the parental strain Wis54-1255. Error bars represent the standard deviation of three replicates.

See also Tables S4–S6.

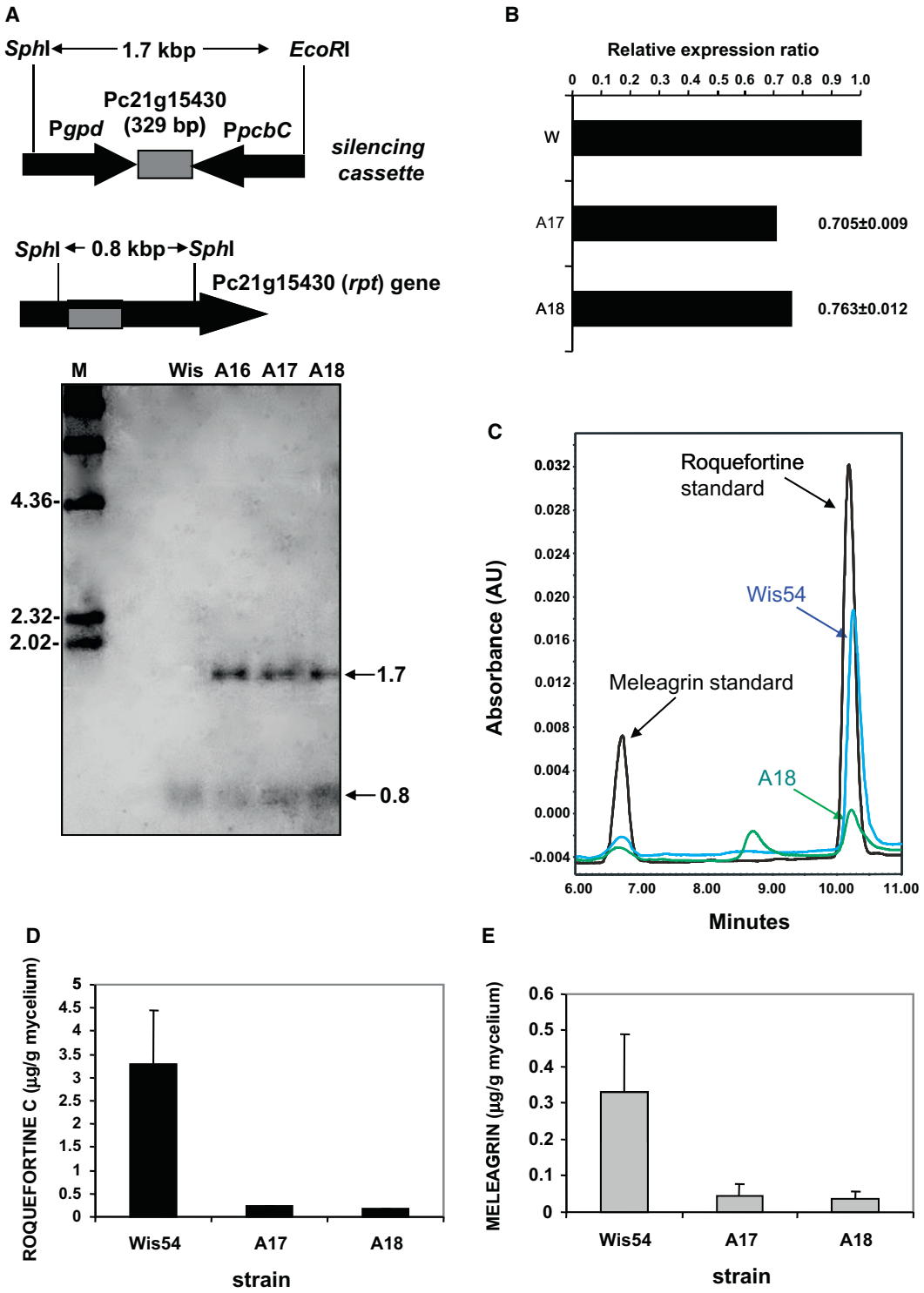

Figure 4. Gene Silencing of Pc21g15430

(A) Southern blot analysis of transformants and the parental *P. chrysogenum* Wis54-1255 (Wis) showing integration of the full silencing cassette (~1.7 kb).

(B) qPCR analysis of the expression of Pc21g15430 in *P. chrysogenum* Wis54-1255 (W) and transformants A17 and A18.

(C) Representative chromatogram showing the meleagrin and roquefortine secreted to the culture medium by transformant A18 and the parental strain Wis54-1255. Pure roquefortine C and meleagrin A standards were added as controls.

(D and E) Roquefortine C and meleagrin-specific production (µg/g dry cells), respectively, by transformants A17, A18, and the parental strain Wis54-1255. Error bars represent the standard deviation of three replicates.

See also Tables S4–S6.

Silencing of the Oxidoreductases Pc21g15460 or Pc21g15470 Reduces the Biosynthesis of Roquefortine C and Meleagrin

Pc21g15460 was silenced using plasmid pJL43RNAi-60 (see Experimental Procedures), which was introduced into the Wis54-1255 strain. Transformants were selected with phleomycin. Southern blotting was carried out in five randomly selected transformants (named D4, D8, D16, D32, and D64) to confirm the integration of the attenuation cassette in the genome and the integrity of the endogenous gene (Figure 5A). Genomic DNA was digested with SphI and EcoRV, which release approximately 1.9 kbp of the attenuation cassette and a 3.3 kbp band including the endogenous gene. The same fragment used for the attenuation of the Pc21g15460 gene was used as probe. Three transformants showed the attenuation cassette, and two of them, transformants D8 and D16, were used for further analyses. Silencing of Pc21g15460 was confirmed in these transformants by qPCR (Figure 5B), and production of roquefortine C and meleagrin was analyzed by HPLC (Figure 5C). In transformants D8 and D16, roquefortine C production was reduced between 3.97 and 17.1 times, respectively (Figure 5D), with respect to the parental strain. Similarly, meleagrin production was reduced in these transformants between 21.1 and 380 times, respectively (Figure 5E), as compared to the parental strain.

Pc21g15470 was also silenced using plasmid pJL43RNAi-70 (see Experimental Procedures). After transformation of the Wis54-1255 strain, transformants were selected using phleomycin. Southern blotting was performed with the DNA (digested with SphI and HindIII) of five randomly selected transformants (named E24, E31, E33, E37, and E40) to confirm the integration of the attenuation cassette in the genome and the integrity of the endogenous gene (Figure 6A). Digestion of the genomic DNA gave rise to a 1.9 kbp band (attenuation cassette) and a 4.3 kbp band (endogenous gene). The same fragment used for the attenuation of the Pc21g15470 gene was used as probe. Three transformants showed the attenuation cassette. Transformants E31 and E40 were selected for further experiments, and silencing of Pc21g15470 was confirmed by qPCR (Figure 6B). Production of roquefortine C and meleagrin was analyzed by HPLC (Figure 6C), indicating that in transformants E31 and E40, roquefortine C yields were reduced between 6.19 and 3.65 times, respectively (Figure 6D), with respect to the parental Wis54-1255 strain. Meleagrin production was reduced in these transformants between 83.4 and 24.1 times, respectively (Figure 6E), as compared to the parental strain.

These results suggest that the two putative oxidoreductases encoded by Pc21g15460 and Pc21g15470 catalyze steps involved in the formation of both roquefortine C and meleagrin (see Discussion).

Late Reaction: Silencing of the Putative Glandicoline B Methyltransferase Leads to Accumulation of Glandicoline B

In order to study whether Pc21g15440 encodes the methyltransferase involved in the conversion of glandicoline B to meleagrin, gene-silencing experiments were carried out. The Wis54-1255 strain was transformed with plasmid pJL43RNAi-*met*. Eight phleomycin-resistant transformants were randomly selected, and the integration of the attenuation cassette (~1.7 kbp) was confirmed by southern blotting after digestion of their genomic DNA with HindIII and SphI (Figure 7A). The same 389 bp internal fragment used for the attenuation of Pc21g15440 was utilized as probe. Two transformants (C25 and C27) showed the correct band corresponding to the full attenuation cassette and were selected for further experiments.

Silencing of the Pc21g15440 gene in transformants C25 and C27 was confirmed by qPCR (Figure 7B), and production of roquefortine C and meleagrin was analyzed by HPLC (Figure 7C). Roquefortine C production in the silenced transformants remained similar to that found in the parental Wis54-1255 strain, whereas meleagrin levels decreased two times in transformant C25 and 3.5 times in transformant C27 (Figures 7D and 7E).

In addition the analysis by Atmospheric Pressure Chemical Ionization Mass Spectrometry (HPLC-MM-ES+APCI) of the peaks obtained in the chromatogram of transformant C27 (data not shown) revealed a molecule with a mass of 419 g/mol that accumulated in a peak that was not detected in the parental Wis54-1255 strain (peak G in Figure 7C). The mass of this molecule coincided with that of glandicoline B, indicating that this intermediate (that is not observed in the parental strain) accumulates in the knockdown mutant due to a lower methylation rate. These results indicate that the conversion of glandicoline B to meleagrin is performed by the methyltransferase encoded by Pc21g15440; therefore, this gene has been named *gmt* for glandicoline methyltransferase.

DISCUSSION

Genes for secondary metabolite biosynthesis and secretion are often clustered in bacteria and filamentous fungi (Martín and Liras, 1989; Keller and Hohn, 1997). Modified cyclodipeptides derived from DKPs are a group of prominent microbial effectors with diverse properties including quorum sensing, invasion processes of animals and plants, cancer chemotherapy, and in the case of dehydrohistidine-containing compounds, inhibition of hemoproteins (Perrin et al., 2009).

NRPSs forming cyclodipeptides consist of two modules, each containing an amino acid A-domain, a carrier domain, and a C-domain catalyzing peptide bond formation. The first C-domain, C1, catalyzes dipeptide formation between two aminoacyl intermediates, whereas a second type of C-domain, C2, promotes cyclization to the DKP. Most work so far has focused on ETPs such as gliotoxin and sirodesmin, and the respective gene clusters have been shown to originate from a progenitor cluster and are found to be scattered throughout various ascomycetes by mechanisms of cluster loss and lateral transfers (Patron et al., 2007). The roquefortine biosynthetic cluster described here includes a clearly different class of dipeptide synthetases. A phylogenetic analysis of CDPSs of the type A-T-C1-A-T-C2 shows an early divergence of: (1) ETP precursor-forming systems, and (2) indole alkaloid type precursor-forming systems of the roquefortine/aszonalenin/fumitremorgin type (Figure S1). Both types of NRPS genes are clustered with a variety of modifying protein genes, most probably being a set of different prenyl transferases (or DMATs). ETP systems share a unique N-methyltransferase differing from those of other NRPS pathways.

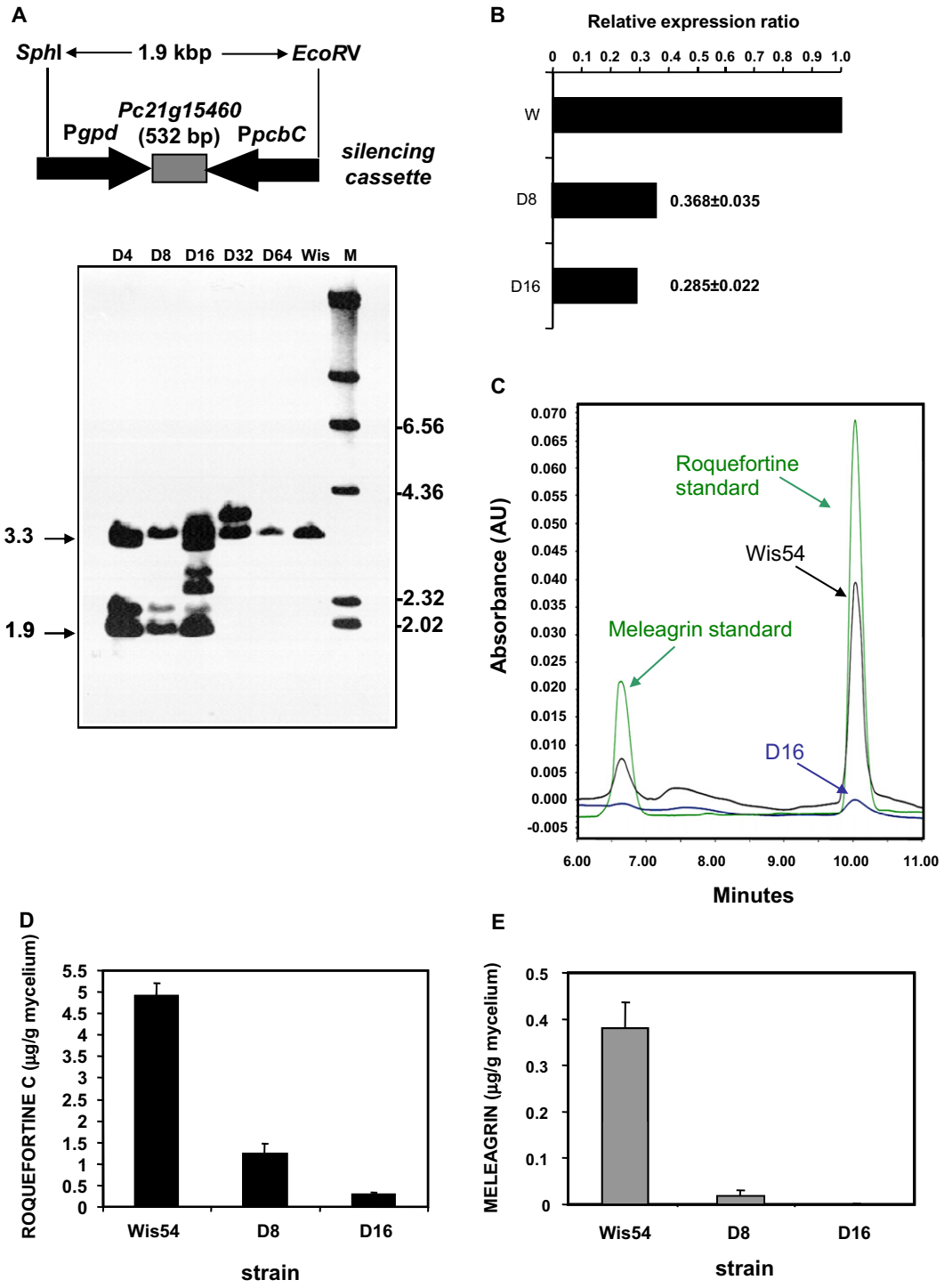

Figure 5. Gene Silencing of Pc21g15460

(A) Southern blot analysis of transformants and the parental *P. chrysogenum* Wis54-1255 (Wis). Transformants D4, D8, and D16 showed integration of the full silencing cassette (~1.9 kbp).

(B) qPCR analysis of the expression of Pc21g15460 in *P. chrysogenum* Wis54-1255 (W) and transformants D8 and D16.

(C) Representative chromatogram showing the meleagrin and roquefortine secreted to the culture medium by transformant D16 and the parental strain Wis54-1255. Pure roquefortine C and meleagrin A standards were added as controls.

(D and E) Roquefortine C and meleagrin-specific production (µg/g dry cells), respectively, by transformants D8, D16, and the parental strain Wis54-1255. Error bars represent the standard deviation of three replicates.

See also Tables S4–S6.

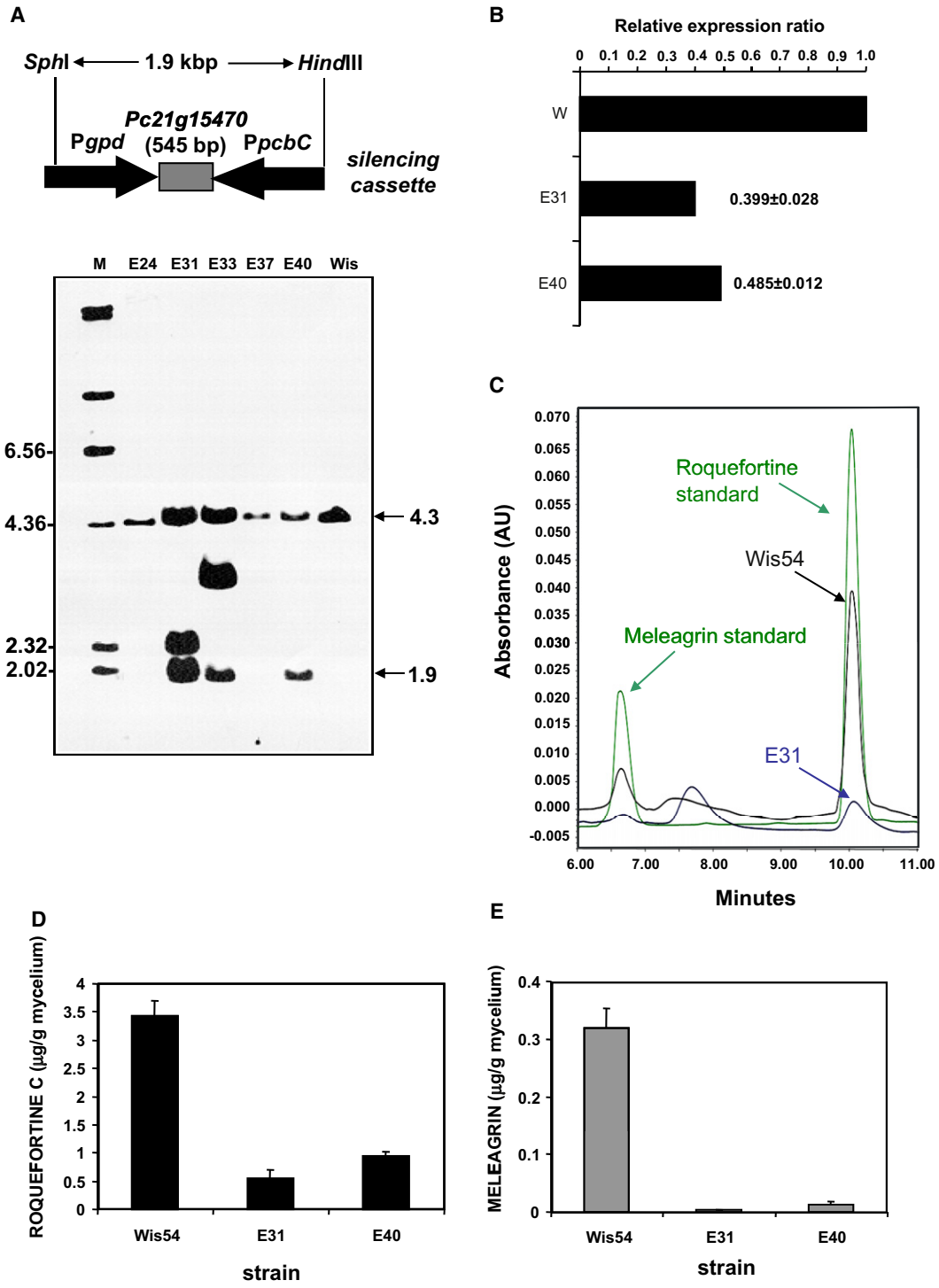

Figure 6. Gene Silencing of Pc21g15470

(A) Southern blot analysis of transformants and the parental *P. chrysogenum* Wis54-1255 (Wis). Transformants E31, E33, and E40 showed integration of the full silencing cassette (~1.9 kbp).

(B) qPCR analysis of the expression of Pc21g15470 in *P. chrysogenum* Wis54-1255 (W) and transformants E31 and E40.

(C) Representative chromatogram showing the meleagrin and roquefortine secreted to the culture medium by transformant E31 and the parental strain Wis54-1255. Pure roquefortine C and meleagrin A standards were added as controls.

(D and E) Roquefortine C and meleagrin-specific production (µg/g dry cells), respectively, by transformants E31, E40, and the parental strain Wis54-1255. Error bars represent the standard deviation of three replicates.

See also Tables S4–S6.

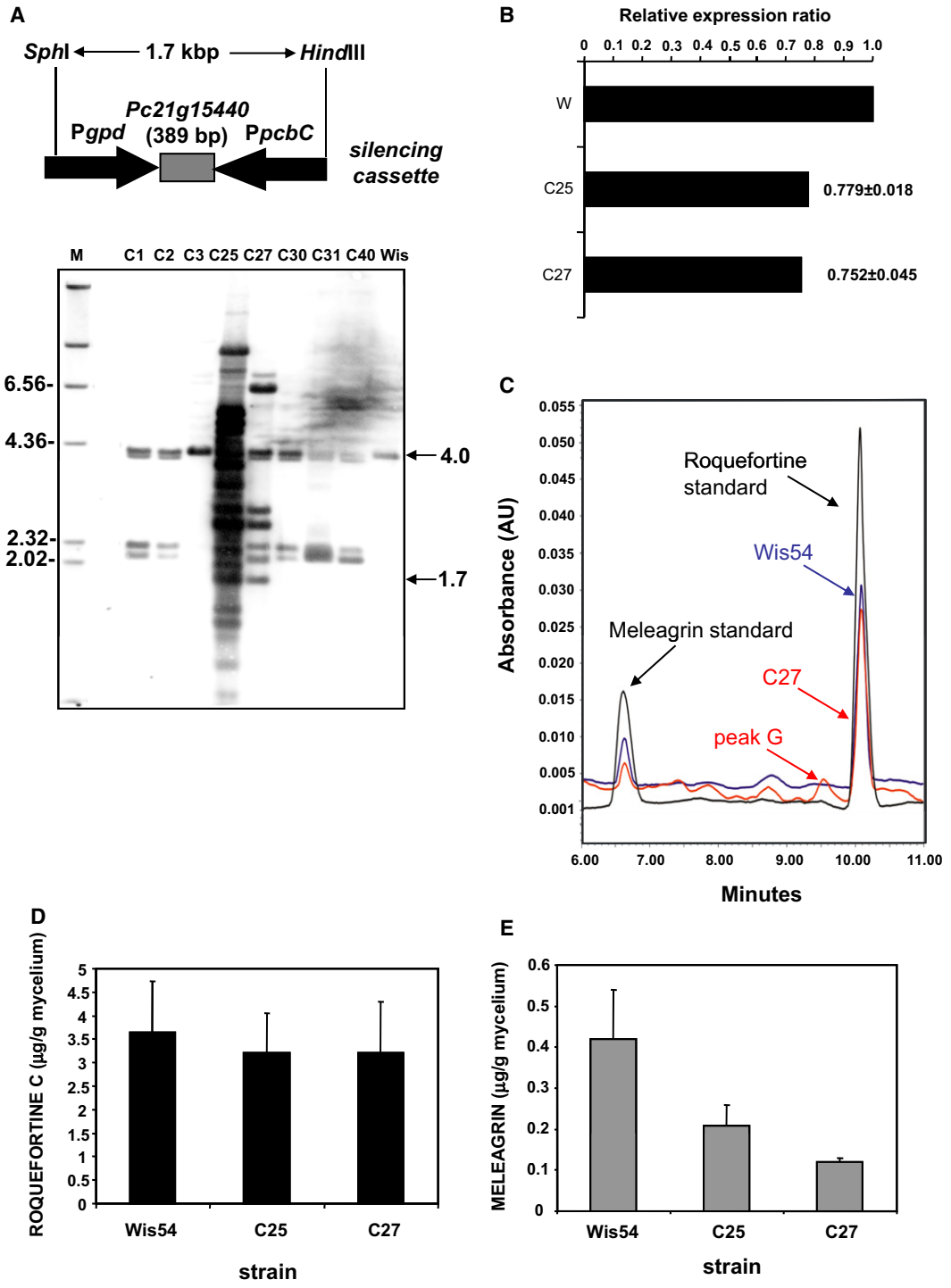

Figure 7. Gene Silencing of Pc21g15440

(A) Southern blot analysis of transformants and the parental *P. chrysogenum* Wis54-1255 (Wis). Transformants C25 and C27 showed the integration of the full silencing cassette (~1.7 kb).

(B) qPCR analysis of the expression of Pc21g15440 in *P. chrysogenum* Wis54-1255 (W) and transformants C25 and C27.

(C) Representative chromatogram showing the meleagrin and roquefortine secreted to the culture medium by transformant C27 and the parental strain Wis54-1255. The peak including the molecule whose mass is coincident with that of glandicoline B is indicated as peak G (retention time 9.55 min).

(D and E) Roquefortine C and meleagrin-specific production (µg/g dry cells), respectively, by transformants C25, C27, and the parental strain Wis54-1255. Error bars represent the standard deviation of three replicates.

See also Tables S4–S6.

Indole alkaloid type of compounds utilize unmodified Trp as one of the amino acids, and in the biosynthetic processes both the respective prenyltransferase and cytochrome P450 enzymes (CYP) catalyze the formation of complex ring systems. In the roquefortine system a variety of products are observed, including roquefortine C, which by oxygenation and ring rearrangement, is transformed to glandicolines A and B, and by methylation is converted to meleagrin. We have shown here by RNAi-silencing techniques that the NRPS Rds, the prenyltransferase Rpt, and two oxidoreductase genes are involved in the biosynthesis of the roquefortine/meleagrin indole alkaloids, whereas the methyltransferase Gmt is specifically involved in the conversion of glandicoline B to meleagrin.

The CDPS Rds belongs phylogenetically to the indole alkaloid NRPS group, which diverges into the fumitremorgin cluster and the roquefortine/aszonalenin cluster (Figure S1). Similarities within the indole alkaloid cluster are fairly low, except for subclusters formed by orthologs. Thus, the closely related *N. fischeri* CDP NFIA_074300 shows 59% amino acid identity, whereas the CDPS Pc21g12630 in the next close subcluster has only 31% identity. Because A-domains of this group activate Trp, we compared substrate signature codes based on the Stachelhaus/Challis algorithm (Table S3). In the 34 amino acid code describing all side chains within 8 Å of the binding pocket of modules 1 and 2 of *N. fischeri*, only two and four residues, respectively, differ from those of *P. chrysogenum* Rds. Besides NFIA_074300, no significant similarity has been found, indicating that the Trp domain of roquefortine and NFIA074300 belong to a subcluster with a unique Trp-binding site. The same holds for the His-activating domain of both CDPSs. BLAST searches comparing A-domains and A-domain specificity regions also failed to identify highly similar structured A-sites. A comparison of the extended signature codes (Rausch et al., 2005) divides the known Trp signatures into a bacterial and a fungal branch; our results indicate that the fungal branch related to indole alkaloid systems subdivides into the roquefortine and the aszonalenin/fumitremorgin type (Figure S1).

The orthologous cluster of the roquefortine biosynthetic genes found in *N. fischeri* is shorter, consisting of orthologs of Pc21g15430 (NFIA_074280, 67% identity to Rpt), Pc21g15470 (NFIA_074290, 60% identity to the cyclodipeptide oxygenase), and Pc21g15480 (NFIA_074300, 59% identity to *Rds*), thus lacking three downstream genes involved in the conversion of roquefortine C to meleagrin. Due to the identical binding site signatures of the NRPS NFIA_074300 and *Rds*, it can be predicted that *N. fischeri* produces also roquefortine or a closely related compound, in addition to verruculogen and fumitremorgin.

The presence of a dehydrohistidine residue in roquefortine C is intriguing. Roquefortine D (3,12-dihydroroquefortine C) contains a histidine moiety in the cyclodipeptide instead of dehydrohistidine. The conversion of roquefortine D to roquefortine C has been suggested (Richard et al., 2004) and is likely to be carried out by cytochrome P450 monoxygenase catalyzing hydroxylation/dehydration. We have not found roquefortine D in the culture medium or cell extracts of *P. chrysogenum*, but it has been reported to be present in small amounts in cultures of *P. roqueforti* (Ohmomo et al., 1978), *P. farinosum* (Kozlovsky et al., 1981), and other plant bulb-infecting *Penicillium* species (Overy et al., 2005). The information available suggests that the roquefortine/meleagrin CDPS has a specificity for histidine, and this amino acid is dehydrogenated or dehydrated at a later stage.

Dehydrohistidine is a rare amino acid present also in oxaline, another member of the roquefortine group of indole alkaloids, and in the novel fungal metabolite phenylahistin, a cytotoxic microtubule-binding agent with potential antitumor applications produced by *Aspergillus ustus* (Kanoh et al., 1999). It is likely that in all these metabolites, dehydrohistidine derives from histidine by a similar mechanism.

One of the proteins of *N. fischeri* homologous to Rpt has been identified recently as a DKP prenyltransferase (AnaPT) involved in the biosynthesis of acetylaszonalenin (Yin et al., 2009a, 2009b). Biochemical evidence suggests that this enzyme belongs to the group of prenyltransferases acting on DKPs with reverse prenylation in position 3 of tryptophan (Table S2 and Figure S2). The similarity of the Rpt gene with that of *N. fischeri* AnaPT supports the conclusion that the roquefortine prenyltransferase belongs to the group of enzymes that catalyzes the reverse prenylation of benzodiazepinedione at position C3 of the indole ring. A phylogenetic analysis of DMAT-like proteins revealed that Rpt clusters with the cyclic dipeptide N-prenyltransferase CdpPT can be considered as reverse prenyltransferases. The prenylation is followed by formation of ring C between the C2 of Trp and the N12 of the DKP ring (Yin et al., 2009a). The evidence in this article indicates that this cyclization is mediated by the N-oxidizing Pc21g15460 oxidoreductase (see below).

The conversion of roquefortine C to other DKP alkaloids in *Penicillium glandicola* was postulated by Reshetilova et al. (1995). The transformation of roquefortine C into glandicoline A involves the introduction of an additional oxygen atom in ring C appearing as a hydroxyl group in glandicoline A, and the rearrangement of the DKP ring of roquefortine C. This reaction is most likely carried out by the monooxygenase Pc21g15450 present in the cloned gene cluster, which closely resembles ftmG (64% identity, 79% similarity at the amino acid level), a P450 monooxygenase catalyzing the introduction of two positionally equivalent hydroxyl groups in fumitremorgin biosynthesis (Kato et al., 2009).

The subsequent conversion of glandicoline A to glandicoline B involves an N-hydroxylation at the nitrogen atom of the indole ring. N-hydroxylases occur in some secondary metabolite gene clusters, although they are very poorly characterized (Bailey and Larson, 1991). The monooxygenase encoded by Pc21g15460 has partial similarity to the maackiain detoxification protein MAK1 (a flavin-dependent monoxygenase). The MAK1 protein of *Nectria haematococca* (Covert et al., 1996) is a flavin containing monooxygenase involved in the conversion of maackiain to 1-hydroxymaackiain. Other N-hydroxylases from *Streptomyces* species, such as the N-hydroxylase involved in desferrioxamine biosynthesis, are also FAD dependent (Challis, 2005), supporting the conclusion that the flavin-dependent MAK1-like protein encoded by Pc21g15460 is the glandicoline N-hydroxylase. In fact silencing of Pc21g15460 had a strong effect on meleagrin production. In addition, silencing of this gene also reduced the levels of roquefortine C, suggesting that the protein encoded by this gene is also involved in the oxidation

of the N atom of ring D of prenylated cyclo-His-Trip that gives rise to roquefortine D.

Our results about the *gmt* gene provide clear evidence for the involvement of this protein in the conversion of glandicoline B into meleagrin (the last step of the pathway). The silenced transformants showed a clearly reduced production of meleagrin but normal levels of roquefortine C. This is the only methyltransferase in the roquefortine C/meleagrin gene cluster, and therefore, its function is clearly assigned. According to these results, we postulate a model pathway for roquefortine and meleagrin biosynthesis (Figure 1B).

The presence in the cluster of an MFS-type transporter containing 12 TMSs similar to the CFP is consistent with the presence of specific transporters in many secondary metabolite gene clusters (reviewed in Martín et al., 2005). The CFP gene (*cfp*) from *C. kikuchii* encodes a 65 kDa MFS protein that is involved in cercosporin secretion (Callahan et al., 1999). MFS transporters show a relatively wide substrate specificity. It is likely that the transporter encoded by Pc21g15420 is involved in the secretion of both roquefortine C and meleagrin.

Based on the evidence obtained, roquefortine C may be considered as an intermediate in the meleagrin biosynthetic pathway (Figure 1B). The limits of the cluster are deduced from previous transcriptomic studies. Genes Pc21g15410 and Pc21g15490 on each side of the cluster are not coregulated with the seven genes of the roquefortine C-meleagrin cluster (van den Berg et al., 2008).

SIGNIFICANCE

Fungal genome sequencing has revealed an unexpected variety of secondary metabolites, mainly of polyketide and nonribosomal peptide origin. This variety stems not only from the large number of biosynthetic clusters but also from the versatility of modifying enzymes. We report here the identification of an indole alkaloid cluster in *P. chrysogenum*, responsible for the production of roquefortine C, glandicolines, and meleagrin, all derived from cyclo-L-His-L-Trp by modification reactions. The cyclodipeptide synthetase belongs to a group of indole alkaloid type two-module NRPSs, which differs from the group of epipolythiodioxopiperazine-related NRPSs. These roquefortine-related NRPSs differ in their unique Trp-binding pocket from related enzymes involved in the biosynthesis of aszonalenins and fumitremorgins. The functions of the modifying enzymes have been deduced from the alkaloid products using mutants silenced in each gene. A prenyltransferase catalyzes the reverse prenylation in R configuration in carbon 3 position of the diketopiperazine, followed by ring closure between C2 and N12. Two oxidoreductases and a cytochrome P450 oxygenase are involved in hydroxylations and dehydrations of the pathway intermediates, and one N-OH methyltransferase leads to meleagrin. The coordinated overexpression of this cluster in industrial *P. chrysogenum* mutant strains indicates that these six genes together with an MFS transporter are responsible for the biosynthesis and secretion of several alkaloids of the roquefortine-meleagrin family due to the multifunctionality of the modifying enzymes.

EXPERIMENTAL PROCEDURES

Fungal Strains and Culture Conditions

P. chrysogenum Wis54-1255 was used as parental strain for the gene-silencing experiments. Fungal spores were obtained from plates of Power medium (Casqueiro et al., 1999) grown for 5 days at 28°C.

Plasmid Constructions for Gene Silencing

Plasmid pJL43-RNAi (Ullán et al., 2008) was used to generate knockdown transformants in different genes of the cluster. It was digested with NcoI for subcloning different inserts, thus giving rise to plasmids pJL43RNAi-*rpt*, pJL43RNAi-*dps*, pJL43RNAi-60, pJL43RNAi-70, and pJL43RNAi-*met* (Table S4).

Transformation of *P. chrysogenum* Protoplasts

P. chrysogenum protoplasts were obtained and transformed as previously described (Cantoral et al., 1987; Díez et al., 1987; Fierro et al., 1993). Transformant clones were selected by resistance to phleomycin (30 μg/ml).

DNA Extraction and Southern Blotting

Spores from *P. chrysogenum* were inoculated into MPPY medium (Fierro et al., 1993). DNA isolation and southern blotting were carried out as described before (Fierro et al., 2006). The same DNA fragments amplified by PCR used to synthesize the gene-silencing constructs (see above) were labeled with digoxigenin (Roche Applied Science) and used as probes.

Complementary DNA Synthesis and qPCR Experiments

Total RNA was quantified in a NanoDrop ND 1000 spectrophotometer (Thermo Scientific). Retrotranscription was carried out with the SuperScript III Reverse Transcriptase (Invitrogen) using 2 μg of total RNA as template and random primers, following manufacturer's instructions.

Gene expression was analyzed by qPCR using the primers listed in Table S5. All reactions were performed in 20 μl reaction volumes that contained 10 μl of SYBR Green PCR master mix (Applied Biosystems), 6.8 μl of H_2O, 0.6 μl of each primer (at a concentration of 10 μM each), and 2 μl of cDNA. Thermocycling conditions were as follows: 10 min at 95°C and 40 cycles of 15 s at 95°C and 1 min at 57°C (the optimal annealing temperature was determined using a range of temperatures from 53°C to 63°C). Appropriate negative controls containing no template DNA (negative control) or total RNA (RT-negative control) were performed. The *actA* gene (encoding the β-actin) was used as internal control for normalization in qPCR conditions. Quantification was carried out with a StepOnePlus™ Real-Time PCR System (Applied Biosystems). Correlation coefficient (R^2), slope, and efficiency of calibration curves obtained for the genes of interest are included in Table S6. The relative expression ratio of each gene was calculated based on the efficiency and ΔCt (between the Wis54-1255 control strain and the mutant) and in comparison to the reference gene (*actA*) following the mathematical model developed by Pfaffl (2001). Results are expressed as the mean value plus the standard deviation of three replicates.

Extraction of Roquefortine C and Meleagrin from *P. chrysogenum*

A suspension containing 10^7 spores/ml obtained from the Wis54-1255 strain and knockdown mutants was spread over a Petri dish-shaped plastic film (gel-drying film; Promega), which was placed on a Petri dish containing 20 ml of YES medium (15% sucrose, 2% yeast extract, 2% agar) and incubated for 10 days at 25°C in the dark. Roquefortine and meleagrin were extracted from the solid culture medium after removal of the plastic film with the mycelia as previously described (Hansen et al., 2005). The protocol included a double extraction with 40 ml dichloromethane for 1 hr in the ultrasonic bath, gentle evaporation to dryness in a vacuum rotary-evaporator, and resuspension in 300 μl of a 2:1 (v/v) methanol-ethanol mixture. Mycelia grown on the plastic film were collected, dried at 85°C for 72 hr, and weighted to calculate the mycotoxin-specific production. Results were provided as the mean value plus standard deviation from three independent measurements.

HPLC Analysis of Roquefortine C and Meleagrin

The extraction solvent was concentrated under vacuum and evaporated to dryness using a SpeedVac SC110 (Savant Instruments, New York). Finally,

1 ml methanol:ethanol ([50:50]vol/vol) was added to each vial to dissolve the extracted compounds. Before HPLC injection, the samples were centrifuged at 13,000 rpm for 2 min, followed by filtration through 0.22 μm filters.

Quantitative determination of meleagrin and roquefortine C was achieved after separation in a XBridge column (2.1 × 150 mm; 3.5 μm) using a Waters Alliance 2695 Separations module with a 2998 photodiode array detector. Elution was performed with water MilliQ plus 0.05% TFA (solvent A) and acetonitrile (solvent B) at a flow rate of 0.3 ml/min and 30°C in the gradient mode from 25% to 40% solvent B in 15 min, followed by 100% B and re-equilibration to initial conditions.

Detection was routinely performed at 304 nm, but for compound identification a wavelength range from 190 to 400 nm was screened. Calibration curves were prepared with the following correlation coefficients: R^2 = 0.9996 for meleagrin, and R^2 = 0.9993 for roquefortine. A standard of pure roquefortine C was kindly provided by A. Fernández, Institute Biomar (León, Spain), and the meleagrin control was obtained from J. David Miller (Ottawa, Canada).

Modeling of Adenylate Domains

The dipeptide synthetase (Pc21g15480) adenylate domains have been aligned to GrsA with Align2D using the program MODELLER (http://salilab.org/modeller). A respective model structure is then calculated by MODELLER with the GrsA structural data (PDB ID: 1Amu). The models have been analyzed by superpositioning with the GrsA structure in the Swiss-PdbViewer DeepView. Substrate-binding pockets were visualized after transfer of the coordinates of AMP and Phe, and replacement by His and Trp, respectively. Substrate conformations have been visualized by PyMOL (http://pymol.sourceforge.net/). Fit of substrates has been investigated considering amino acid side chains within 4 Å distance for possible interactions. The models have been optimized by variations of the rotational angles of the side chains to avoid steric hindrance and direct neighborhood of polar and unpolar groups, and to permit the formation of H- bonding. This approach permits a clear decision with respect to the charged His and the large Trp as substrates.

SUPPLEMENTAL INFORMATION

Supplemental Information includes two figures and six tables and can be found with this article online at doi:10.1016/j.chembiol.2011.08.012.

ACKNOWLEDGMENTS

This research was supported by a project of the European Union (Eurofungbase LSSG-CT-2005-018964). S.M.A. was supported by a Torres Quevedo Contract (PTQ06-2-0113) of the Ministry of Science and Innovation (Madrid). M.A.F.-B. received a PhD fellowship of the Diputación de León (Spain). We thank A. Fernández (Instituto Biomar, León, Spain) for a sample of pure roquefortine C and J.D. Miller (Ottawa, Canada) for a sample of pure meleagrin. Authors also wish to thank M.T. López, R. Álvarez, and C.M. Vicente for help with the qPCR experiments.

Received: February 9, 2010
Revised: August 25, 2011
Accepted: August 25, 2011
Published: November 22, 2011

REFERENCES

Bailey, B.A., and Larson, R.L. (1991). Maize microsomal benzoxazinone N-monooxygenase. Plant Physiol. *95*, 792–796.

Barrow, K.D., Colley, P.W., and Tribe, D.E. (1979). Biosynthesis of the neurotoxin alkaloid roquefortine. J. Chem. Soc. Chem. Commun. 225–226.

Callahan, T.M., Rose, M.S., Meade, M.J., Ehrenshaft, M., and Upchurch, R.G. (1999). CFP, the putative cercosporin transporter of *Cercospora kikuchii*, is required for wild type cercosporin production, resistance, and virulence on soybean. Mol. Plant Microbe Interact. *12*, 901–910.

Cantoral, J.M., Díez, B., Barredo, J.L., Álvarez, E., and Martín, J.F. (1987). High frequency transformation of *Penicillium chrysogenum*. Nat. Biotechnol. *5*, 494–497.

Casqueiro, J., Bañuelos, O., Gutiérrez, S., Hijarrubia, M.J., and Martín, J.F. (1999). Intrachromosomal recombination between direct repeats in *Penicillium chrysogenum*: gene conversion and deletion events. Mol. Gen. Genet. *261*, 994–1000.

Challis, G.L. (2005). A widely distributed bacterial pathway for siderophore biosynthesis independent of nonribosomal peptide synthetases. ChemBioChem *6*, 601–611.

Cole, R.J., Dorner, J.W., Cox, R.H., and Raymond, L.W. (1983). Two classes of alkaloid mycotoxins produced by *Penicillium crustosum* thom isolated from contaminated beer. J. Agric. Food Chem. *31*, 655–657.

Covert, S.F., Enkerli, J., Miao, V.P., and VanEtten, H.D. (1996). A gene for maackiain detoxification from a dispensable chromosome of *Nectria haematococca*. Mol. Gen. Genet. *251*, 397–406.

Díez, B., Álvarez, E., Cantoral, J.M., Barredo, J.L., and Martín, J.F. (1987). Selection and characterization of pyrG mutants of *Penicillium chrysogenum* lacking orotidine-5′-phosphate decarboxylase and complementation by the pyr4 gene of *Neurospora crassa*. Curr. Genet. *12*, 277–282.

Fierro, F., Gutiérrez, S., Díez, B., and Martín, J.F. (1993). Resolution of four large chromosomes in penicillin-producing filamentous fungi: the penicillin gene cluster is located on chromosome II (9.6 Mb) in *Penicillium notatum* and chromosome I (10.4 Mb) in *Penicillium chrysogenum*. Mol. Gen. Genet. *241*, 573–578.

Fierro, F., García-Estrada, C., Castillo, N.I., Rodríguez, R., Velasco-Conde, T., and Martín, J.F. (2006). Transcriptional and bioinformatic analysis of the 56.8 kb DNA region amplified in tandem repeats containing the penicillin gene cluster in *Penicillium chrysogenum*. Fungal Genet. Biol. *43*, 618–629.

Finoli, C., Vecchio, A., Galli, A., and Dragoni, I. (2001). Roquefortine C occurrence in blue cheese. J. Food Prot. *64*, 246–251.

García-Rico, R.O., Fierro, F., Mauriz, E., Gómez, A., Fernández-Bodega, M.A., and Martín, J.F. (2008). The heterotrimeric Galpha protein pga1 regulates biosynthesis of penicillin, chrysogenin and roquefortine in *Penicillium chrysogenum*. Microbiology *154*, 3567–3578.

Godio, R.P., and Martín, J.F. (2009). Modified oxidosqualene cyclases in the formation of bioactive secondary metabolites: biosynthesis of the antitumor clavaric acid. Fungal Genet. Biol. *46*, 232–242.

Gorst-Allman, C.P., Steyn, P.S., and Vleggaar, R. (1982). The biosynthesis of roquefortine. An investigation of acetate and mevalonate incorporation using high field n.m.r. spectroscopy. J. Chem. Soc. Chem. Commun. 652–653.

Häggblom, P. (1990). Isolation of roquefortine C from feed grain. Appl. Environ. Microbiol. *56*, 2924–2926.

Hansen, M.E., Andersen, B., and Smedsgaard, J. (2005). Automated and unbiased classification of chemical profiles from fungi using high performance liquid chromatography. J. Microbiol. Methods *61*, 295–304.

Jarvis, B.B. (2003). Analysis for mycotoxins: the chemist's perspective. Arch. Environ. Health *58*, 479–483.

Jarvis, B.B., and Miller, J.D. (2005). Mycotoxins as harmful indoor air contaminants. Appl. Microbiol. Biotechnol. *66*, 367–372.

Jiang, Z.D., and An, Z. (2000). Bioactive fungal natural products through classic and biocombinatorial approaches. In Studies in Natural Products Chemistry; Bioactive Natural Products (Part C), *Volume 22*, A.U. Rahman, ed. (New York: Elsevier), pp. 245–272.

Kanoh, K., Kohno, S., Katada, J., Takahashi, J., and Uno, I. (1999). (-)-Phenylahistin arrests cells in mitosis by inhibiting tubulin polymerization. J. Antibiot. *52*, 134–141.

Kato, N., Suzuki, H., Takagi, H., Asami, Y., Kakeya, H., Uramoto, M., Usui, T., Takahashi, S., Sugimoto, Y., and Osada, H. (2009). Identification of cytochrome P450s required for fumitremorgin biosynthesis in *Aspergillus fumigatus*. ChemBioChem *10*, 920–928.

Keller, N.P., and Hohn, T.M. (1997). Metabolic pathway gene clusters in filamentous fungi. Fungal Genet. Biol. *21*, 17–29.

Kimura, Y., Hamasaki, T., Nakajima, H., and Isogai, A. (1982). Structure of aszonalenin, a new metabolite of *Aspergillus zonatus*. Tetrahedron Lett. *23*, 225–228.

Kosalková, K., García-Estrada, C., Ullán, R.V., Godio, R.P., Feltrer, R., Teijeira, F., Mauriz, E., and Martín, J.F. (2009). The global regulator LaeA controls

penicillin biosynthesis, pigmentation and sporulation, but not roquefortine C synthesis in *Penicillium chrysogenum*. Biochimie *91*, 214–225.

Kozlovsky, A.G., Solovieva, T.F., Reshetilova, T.A., and Skryabin, G.K. (1981). Biosynthesis of roquefortine and 3,12-dihydroroquefortine by the culture *Penicillium farinosum*. Cell. Mol. Life Sci. *37*, 472–473.

Lautru, S., and Challis, G.L. (2004). Substrate recognition by nonribosomal peptide synthetase multi-enzymes. Microbiology *150*, 1629–1636.

Li, S.M. (2009). Evolution of aromatic prenyltransferases in the biosynthesis of indole derivatives. Phytochemistry *70*, 1746–1757.

Martín, J.F., Casqueiro, J., and Liras, P. (2005). Secretion systems for secondary metabolites: how producer cells send out messages of intercellular communication. Curr. Opin. Microbiol. *8*, 282–293.

Martín, M.F., and Liras, P. (1989). Organization and expression of genes involved in the biosynthesis of antibiotics and other secondary metabolites. Annu. Rev. Microbiol. *43*, 173–206.

Möller, T., Akerstrand, K., and Massoud, T. (1997). Toxin-producing species of *Penicillium* and the development of mycotoxins in must and homemade wine. Nat. Toxins *5*, 86–89.

Ohmomo, S. (1982). Indole alkaloids produced by *Penicillium roqueforti*. J. Antibact. Antifung. Agents *10*, 253–264.

Ohmomo, S., Kitamoto, H.K., and Nakajima, T. (1994). Detection of roquefortines in *Penicillium roqueforti* isolated from moulded maize silage. J. Sci. Food Agric. *64*, 211–215.

Ohmomo, S., Oguma, K., Ohashi, T., and Abe, M. (1978). Isolation of a new indole alkaloid, roquefortine D, from the cultures of *Penicillium roqueforti*. Agric. Biol. Chem. *42*, 2387–2389.

Overy, D.P., Nielsen, K.F., and Smedsgaard, J. (2005). Roquefortine/oxaline biosynthesis pathway metabolites in *Penicillium* ser. *Corymbifera*: in planta production and implications for competitive fitness. J. Chem. Ecol. *31*, 2373–2390.

Patron, N.J., Waller, R.F., Cozijnsen, A.J., Straney, D.C., Gardiner, D.M., Nierman, W.C., and Howlett, B.J. (2007). Origin and distribution of epipolythiodioxopiperazine (ETP) gene clusters in filamentous ascomycetes. BMC Evol. Biol. *7*, 174.

Perrin, L., André, F., Aninat, C., Ricoux, R., Mahy, J.P., Shangguan, N., Joullié, M.M., and Delaforge, M. (2009). Intramolecular hydrogen bonding as a determinant of the inhibitory potency of N-unsubstituted imidazole derivatives towards mammalian hemoproteins. Metallomics *1*, 148–156.

Pfaffl, M.W. (2001). A new mathematical model for relative quantification in real-time RT-PCR. Nucleic Acids Res. *29*, e45.

Rausch, C., Weber, T., Kohlbacher, O., Wohlleben, W., and Huson, D.H. (2005). Specificity prediction of adenylation domains in nonribosomal peptide synthetases (NRPS) using transductive support vector machines (TSVMs). Nucleic Acids Res. *33*, 5799–5808.

Reshetilova, T.A., Vinokurova, N.G., Khmelenina, V.N., and Kozlovsky, A.G. (1995). The role of roquefortine in the synthesis of alkaloids meleagrin, glandicolines A and B, and oxaline in fungi *Penicillium glandicola* and *P. atramentosum*. Mikrobiology (Moscow) *64*, 27–29.

Richard, D.J., Schiavi, B., and Joullié, M.M. (2004). Synthetic studies of roquefortine C: synthesis of isoroquefortine C and a heterocycle. Proc. Natl. Acad. Sci. USA *101*, 11971–11976.

Rundberget, T., Skaar, I., and Flåøyen, A. (2004). The presence of *Penicillium* and *Penicillium* mycotoxins in food wastes. Int. J. Food Microbiol. *90*, 181–188.

Schwecke, T., Göttling, K., Durek, P., Dueñas, I., Käufer, N.F., Zock-Emmenthal, S., Staub, E., Neuhof, T., Dieckmann, R., and von Döhren, H. (2006). Nonribosomal peptide synthesis in *Schizosaccharomyces pombe* and the architectures of ferrichrome-type siderophore synthetases in fungi. ChemBioChem *7*, 612–622.

Scott, P.M., and Kennedy, P.C. (1976). Analysis of blue cheese for roquefortine and other alkaloids from *Penicillium roqueforti*. J. Agric. Food Chem. *24*, 865–868.

Stocking, E.M., Williams, R.M., and Sanz-Cervera, J.F. (2000). Reverse prenyl transferases exhibit poor facial discrimination in the biosynthesis of paraherquamide A, brevianamide A, andaustamide. J. Am. Chem. Soc. *122*, 9089–9098.

Ullán, R.V., Godio, R.P., Teijeira, F., Vaca, I., García-Estrada, C., Feltrer, R., Kosalkova, K., and Martín, J.F. (2008). RNA-silencing in *Penicillium chrysogenum* and *Acremonium chrysogenum*: validation studies using beta-lactam genes expression. J. Microbiol. Methods *75*, 209–218.

van den Berg, M.A., Albang, R., Albermann, K., Badger, J.H., Daran, J.M., Driessen, A.J., Garcia-Estrada, C., Fedorova, N.D., Harris, D.M., Heijne, W.H., et al. (2008). Genome sequencing and analysis of the filamentous fungus *Penicillium chrysogenum*. Nat. Biotechnol. *26*, 1161–1168.

Vinokurova, N.G., Boĭchenko, L.V., and Arinbasarov, M.U. (2003). [Formation of alkaloids from *Penicillium* species fungi during growth on wheat kernels]. Prikl. Biokhim. Mikrobiol. *39*, 457–460.

Wagener, R.E., Davis, N.D., and Diener, U.L. (1980). Penitrem A and roquefortine production by *Penicillium commune*. Appl. Environ. Microbiol. *39*, 882–887.

Wakana, D., Hosoe, T., Itabashi, T., Nozawa, K., Kawai, K., Okada, K., Campos-Takaki, G.M., Yaguchi, T., and Fukushima, K. (2006). Isolation of isoterrein from *Neosartorya fischeri*. Mycotoxins *56*, 3–6.

Williams, R.M., Stocking, E.M., and Sanz-Cervera, J.F. (2000). Biosynthesis of prenylated alkaloids derived from tryptophan. Top. Curr. Chem. *209*, 97–173.

Yin, W.B., Cheng, J., and Li, S.M. (2009a). Stereospecific synthesis of aszonalenins by using two recombinant prenyltransferases. Org. Biomol. Chem. *7*, 2202–2207.

Yin, W.B., Grundmann, A., Cheng, J., and Li, S.M. (2009b). Acetylaszonalenin biosynthesis in *Neosartorya fischeri*. Identification of the biosynthetic gene cluster by genomic mining and functional proof of the genes by biochemical investigation. J. Biol. Chem. *284*, 100–109.

Yu, J.H., Butchko, R.A., Fernandes, M., Keller, N.P., Leonard, T.J., and Adams, T.H. (1996). Conservation of structure and function of the aflatoxin regulatory gene *aflR* from *Aspergillus nidulans* and *A. flavus*. Curr. Genet. *29*, 549–555.